International Conference on Space Optics—ICSO 2004

Toulouse, France

30 March–2 April 2004

Edited by Josiane Costeraste and Errico Armandillo

Miniature high-performance infrared spectrometer for space applications

Roman V. Kruzelecky, Emile Haddad, Brian Wong, Denis Lafrance, et al.

esa icso proceedings cnes

International Conference on Space Optics — ICSO 2004, edited by Errico Armandillo, Josiane Costeraste, Proc. of SPIE Vol. 10568, 105680Q · © 2004 ESA and CNES
CCC code: 0277-786X/17/$18 · doi: 10.1117/12.2307999

Miniature High-Performance Infrared Spectrometer for Space Applications

Roman V. Kruzelecky[(1)], Emile Haddad[(1)], Brian Wong[(1)], Denis Lafrance[(1)], and Wes Jamroz[(1)]

Asoke K. Ghosh[(2)], Wanping Zheng[(2)] and Linh Phong[(2)]

[(1)]*MPB Communications Inc. , 151 Hymus, Pointe Claire, Quebec, Canada H9R-1E9; E-mail: emile.haddad@mpbc.ca*
[(2)]*Canadian Space Agency, 6767 Route de l'Aéroport, Saint Hubert Quebec, Canada, J3Y-8Y9*

ABSTRACT

Infrared spectroscopy probes the characteristic vibrational and rotational modes of chemical bonds in molecules to provide information about both the chemical composition and the bonding configuration of a sample. The significant advantage of the Infrared spectral technique is that it can be used with minimal consumables to simultaneously detect a large variety of chemical and biochemical species with high chemical specificity. To date, relatively large Fourier Transform (FT-IR) spectrometers employing variations of the Michelson interferometer have been successfully employed in space for various IR spectroscopy applications. However, FT-IR systems are mechanically complex, bulky (> 15 kg), and require considerable processing. This paper discusses the use of advanced integrated optics and smart optical coding techniques to significantly extend the performance of miniature IR spectrometers by several orders of magnitude in sensitivity. This can provide the next-generation of compact, high-performance IR spectrometers with monolithically integrated optical systems for robust optical alignment. The entire module can weigh under 3 kg to minimize the mass penalty for space applications. Miniaturized IR spectrometers are versatile and very convenient for small and micro satellite based missions. They can be dedicated to the monitoring of the CO_2 in an Earth Observation mission, to Mars exobiology exploration, as well as to vital life support in manned space system; such as the cabin air quality and the quality of the recycled water supply.

1. INTRODUCTION

The detection and identification of molecular structures is a vital component of Earth observation and space exploration for planetary atmospheric studies, planetary geology, and astrobiology [1]. It is also an important requirement for manned missions in space for the monitoring of vital life-support systems such as water and air recirculation systems [2]. IR spectroscopy is of great benefit for space a in the search for biomarkers, planetary geology and extra-terrestrial life. It is the IR spectral signatures of various hydrocarbon chains that can provide more definitive information. Table 1 presents the spectral resolution and the Signal/Noise ratio (SNR) requirements for some potential space applications of IR spectroscopy.

Table 1: Potential space applications of IR spectroscopy.

Application	Spectral Resolution	SNR
Atmospheric chemistry	< 0.1 nm	200-300
Stratospheric aerosols	1 - 5 nm	$> 10^3$
Nadir atmospheric greenhouse gas distributions	0.1 to 1 nm	$> 10^4$
Planetary and terrestrial geological surveys	5 to 10 nm	$> 10^4$
Insitu monitoring of scientific experiments in space	5 to 10 nm	$> 10^4$
Insitu sample analysis on planetary landers and rovers	5 to 10 nm	$> 10^4$
Monitoring of life-support systems for manned missions in space.	5 to 10 nm (liquid) 1 to 5 nm (gas)	10^5-10^6
Biohazard detection, biomarker detection	5 to 10 nm	$> 10^6$ (trace-ppb)

To date, relatively large FT-IR spectrometers employing variations of the Michelson interferometer have been employed for various IR spectroscopy applications in space [1,3,4]. FT-IR systems have two main advantages over dispersive and filter instruments:

(1) a multiplex SNR since the detector views all the wavelengths simultaneously

(2) enhanced light gathering capability since the aperture size is much larger than in dispersive instruments.

However, FT-IR systems also have a number of shortcomings: the mechanical complexity, and the resultant high cost, the precision of alignment and translation. Current proposed systems [5] based on FT-IR are quite massive (>30 kg), and the measurement process requires measurement data filtering, apodizing and an inverse Fourier transform. Although they can be very accurate in terms of the absolute wavelength, they are less accurate for the absolute signal intensity. Table 2 presents example of the spectral ranges of some greenhouse trace gases, that can be detected using IR spectrometers.

Table 2: Spectral bands that can used to monitor greenhouse gases.

Gas	Absorption Peak:	Absorption Strength Sj	Atmospheric Lifetime (years)	Altitude Range (km)
H_2O	**1.87**	**9 10^{-21}**	days	10 to 80
	2.7	2 10^{-19}		
	6.2	2 10^{-19}		
CO_2	**1.58**		Monthly variation terrestrial sinks and sources.	10 to 100
	2.05			
	4.3	2.5 10^{-18}		
CO	**2.35**	2 10^{-21}	Several months, conversion to CO_2	10 to 100
	4.72	3 10^{-19}		
CH_4	2.25		8-12	10 to 75
	3.25	1 10^{-19}		
	7.66	8 10^{-20}		
NO	**2.67**	1 10^{-21}		10 to 50
	5.24	2 10^{-20}		
N_2O	**2.86**		120 years, atmospheric sinks	10 to 55
	3.88			
	4.5	1 10^{-18}		
	7.78	1.5 10^{-19}		
NO_2	**3.46**	4 10^{-21}		10 to 45
	6.17	2 10^{-19}		

MPB Communications Inc. has advanced its IOSPEC technology (patent-pending) for miniature integrated IR spectrometers to provide high performance comparable to large bench-top FT-IR systems but in a very compact and ruggedized footprint [6,7]. IOSPEC [7], for **I**ntegrated **O**ptical **Spec**trometer, employs a broad-band IR slab-waveguide structure to integrate an input IR fiber or slit, a concave reflection grating, and a linear detector array at the optical output plane, in a compact, monolithic structure. Light is coupled into the spectrometer either directly through a miniature slit, or through a suitable IR fiber array. This precisely defines the position of the diffracted signal at the output focal plane, providing very stable long-term optical alignment. The optical signal is guided within the slab waveguide onto a master blazed grating structure that also serves as a concave reflector. The precision master grating, formed using batch microfabrication techniques, provides diffraction efficiencies approaching theoretical limits (> 85% peak diffraction efficiency) with low background signal scattering (<0.05%). Additional integrated optics assists to linearize the output focal plane, as wide as 20 mm, and to focus the dispersed signal onto the detector array.

In dispersive spectrometers such as IOSPEC, higher spectral resolution is obtained by using a narrower input slit width, which limits the input optical collection efficiency, reducing the attainable SNR. This can be solved by Hadamard transform (HT), that employs binary weighting to multiplex either the optical input signal or the output signal of a dispersive spectrometer [8]. The single narrow input slit is replaced by an array of N_i programmable shutters. This array of shutters is employed to code the optical input to the spectrometer. This technique can provide the same advantages as a Michelson interferometer relative to a simple grating spectrometer; namely Fellgett's advantage of measuring radiation at several wavelengths simultaneously and a large effective input aperture. The binary-coded optical output is deconvolved using a mathematical model much simpler than a Fourier inverse transform.

Early Hadamard Transform spectrometers, operating in the visible spectral range, were first realized in the early 1970's [9]. They typically employed arrays of slits on a rotary wheel that were mechanically positioned to obtain the Hadamard optical code, causing significant problems associated with the mechanical positioning and alignment of the Hadamard mask. Recently Hammaker [10] employed MEMS-based digital micro-mirror arrays (DMA) to provide optical multiplexing between the output plane of a bulk-optic diffraction grating and a single detector. He developed a HT spectrometer operating in the 1 to 1.6 μm spectral range using a 800 element DMA to multiplex the diffracted output signal from a bulk-optic grating spectrometer to a single InGaAs detector. The DMA could also be programmed to simulate a classical dispersive spectrometer with a single output slit. Hammaker [10] observed an improvement in the SNR by a factor of 12 for the HT mode of operation (coded multiplexed output of multiple wavelengths).

This paper describes a novel, high-performance "next-generation" miniature integrated spectrometer that merges advanced input optical coding techniques with the existing IOSPEC^{TM} technology to yield comparable or better SNR capabilities than FT-IR instruments. The technology has tremendous applications for space to reduce the cost and size of current spectral instruments, as well as to enable new opportunities for planetary exploration and to improve the safety of manned spacecraft.

2. MINIATURE INTEGRATED IR SPECTROMETER

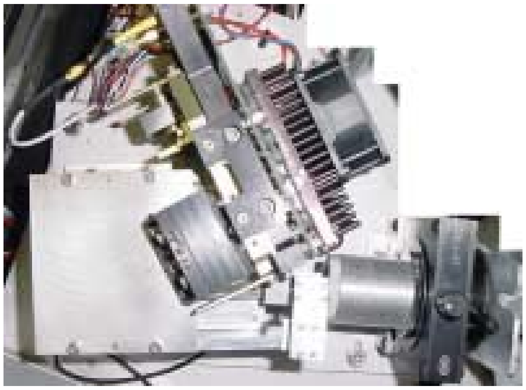

Fig. 1: Photograph of current IOSPEC module weighing under 2 kg including input optics and cooled detector array.

The 1.2 to 5 µm IOSPEC integrated optical spectrometer has been packaged in a compact module, as shown in fig. 1, that is only about 20 x 20 x 15 cm in size and weighs under 2 kg. The current spectrometer is optimized to operate with small light sources such as tungsten lamps.

IOSPEC employs an electronically-scanned linear detector array that can provide relatively high spectral scan rates, exceeding several hundred scans per second, to facilitate a relatively high sample throughput. The elimination of moving components and integration of the optical system provides more reliable long-term performance in non-ideal environments. To date, IOSPEC has been employed with 256 channel PbS and PbSe detector arrays, the detector cooling to about 250K has been provided using a dual-stage thermo-electric cooler requiring about 5 W.

Proprietary (patent-pending) active smart-signal processing and averaging algorithms have been developed that facilitate a significant increase in the attainable SNR for multiplexed linear detector arrays. Using this new technology, the net system noise with the PbSe detector could be reduced to below +/- 1 mV, after a similar total measurement time of 1 second; an order of magnitude improvement. Increasing the processing time yielding further reductions in the signal variation. After a net measurement time of about 10 sec., a SNR of ~25,000 for transmittance measurements using the PbSe arrays and ~ 250,000 for PbS arrays were obtained.

Fig. 2 shows the measured peak-to-peak signal variation for a 256 channel PbS detector array at 260 K versus the number of scans processed using the smart averaging technique. The current version of the active smart processing also includes the optical signal source noise and drift. If measurement time is not critical, then very high SNR is feasible.

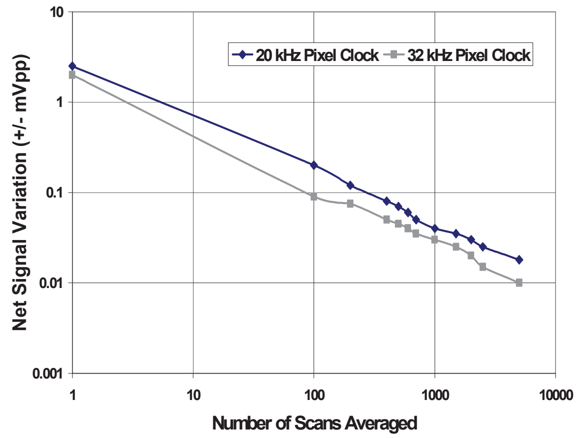

Figure 2: Net signal variation versus the number of sequential scans averaged using active smart signal processing.

3. BINARY OPTICAL CODING

MPB and CSA are developing proprietary algorithms to binary code the optical input to diffractive spectrometers such as IOSPEC to further improve the attainable SNR and spectral resolution. The traditional single input slit is replaced by an N_s array ($N_s \geq 8$) of programmable slits. This increases the effective input aperture by a factor of $N_s/2$, resulting in an unrestricted input aperture for diffractive spectrometers. The optical coding provides a further theoretical gain in SNR by a factor of $N_s^{0..5}/2$, due to input data multiplexing and redundancy. The actual processing combines the smart averaging algorithms with the binary coding to provide a further order-of magnitude improvement in the SNR than is possible using traditional Hadamard transform techniques alone.

Table 3 compares three potential methodologies: thin-film smart materials, MEMS micro-mirrors, and MEMS microlouvers. Individual MEMS tunable micro-optics are typically limited in size to several hundred microns. Thus, an array of them would be required for each slit position in order to provide the desired aperture height. MEMS micromirrors operate in reflection, and therefore, cannot be easily integrated directly with the input of the IOSPEC integrated-optic spectrometer. One drawback with the MEMS programmable micro-optics is the achievable packing density due to the area required for the mechanical drives and microactuators. This will impose some restrictions on the achievable input aperture throughput.

Table 3: Comparison of three miniaturization techniques for optical coding.

Method	Thin-Film Smart Material	MEMS microMirror	MEMS microLouver
Mass	Minimal	Moderate	Moderate
Slit Height	Unlimited	250 µm x n mirrors	250 µm
Packing density	High	> 80%	< 50 %
Optical scattering vs. spectrometer	Minimal	Medium light scatter toward	Moderate, light scatter away
Shutter/Spectro coupling	Can be integrated	Free Space	Can be integrated
Cost	Moderate	High to customize	High to develop
Switching Time	1 to 5 ms, (micro heater) < 1 µs using field-effect	5 ms	Mass dependent, typical 5 ms.
Zero (blocking) state	T≈0 %	T≈5 %	T≈0 %
Reliability	High: no moving components	Mechanical wear, Stickage	Mechanical wear, Stickage
Complexity	Multi-layer thin-film		
Maturity	Voltage control needs development	Micromirrors commercially available	Requires development

One potential solution to the realization of a programmable array of optical shutters is the use of smart coatings that exhibit a metal-insulator transition. This has significant benefits in terms of the mechanical simplicity, reliability, achievable packing density, and the achievable optical performance. The long (2-5 mm), narrow (50 to 100 µm) shutters required for the input coding are readily achievable using established lithography techniques to pattern the smart coating.

The smart coating is based on VO_2 that exhibits one of the largest observed variations in electrical and optical characteristics due to the metal-insulator transition at 341°K. The metal-insulator transition in VO_2 [11] is associated with a change in structure from a tetragonal rutile stucture with highly reflective metallic characteristics above the transition temperature, to a monoclinic structure with optically-transmissive insulator-like characteristics below the transition temperature. The VO_2 is a stoichiometric oxide, it is relatively resistant to atomic oxygen, as has been verified using test facilities at the CSA.

The metal-insulator transition in VO_2 can be triggered using an applied electric field, at room temperature [12]. The switching characteristics of the electrical current using the VO_2 in a Micro structure configuration indicates that the driving mechanism is an electric field effect, the power requirements are moderate, and power is mainly required during the switching.

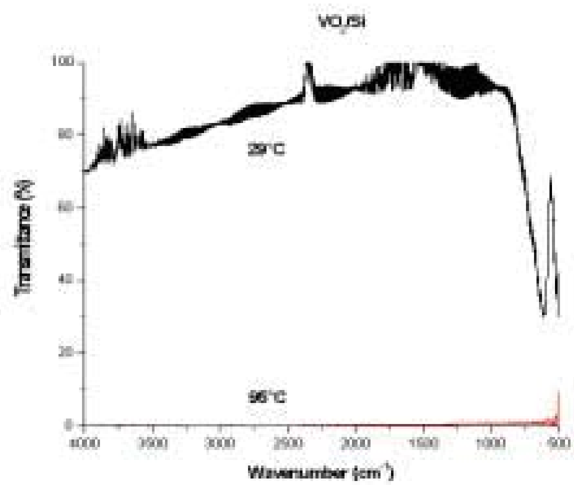

Fig. 3: FT-IR optical transmittance of MPB VO_2 on Si in the insulating (29°C) and metallic (95°C) states.

Various thin-film alloys based on the VO_2 material system have been developed for use as a thin-film smart thermal radiator by MPB [13]. However, this technology can also be applied to provide programmable optical mirrors and shutters. Fig. 3 shows the IR transmission characteristics of a 150 nm thick VO_2 coating deposited by reactive laser ablation onto polished single-crystal Si, as measured using a FT-IR spectrometer. The smart material system can exhibit relatively high broad-band optical transmittance characteristics in the insulating state, typically exceeding 65% from the NIR near 1.2 µm to beyond 14 µm in the far infrared. In the metallic state, the system exhibits correspondingly high metallic reflectivity.

Active voltage control of the optical switching VO_2 system is under development at MPB, using a simple sandwich electrode structure. The structure can be deposited either on a quartz or Si substrate. Fig. 4 shows the variation of an optical signal at 1.55 µm, as provided by a laser diode source, versus the applied voltage to the thin-film structure. The switching voltage was only about 3.5 V. The observed "on/off" switching ratio in transmittance exceeded 35 dB.

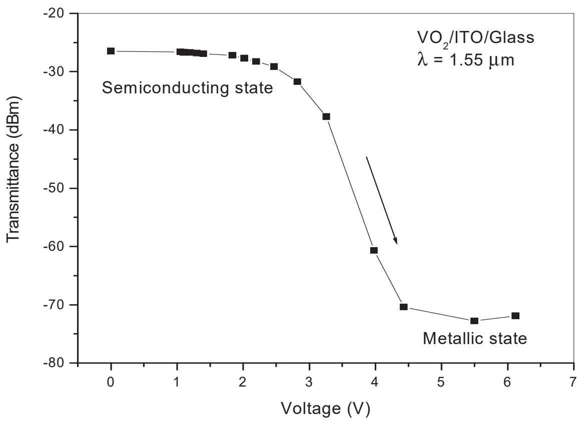

Fig. 4: Voltage-controlled switching of a laser-diode signal at 1.55 µm using a sandwich electrode structure containing VO_2 as the electrochromic layer.

Work is currently underway to develop a 16 element shutter array that can be integrated at the input of the current 1 to 5 µm IOSPEC spectrometer. A preliminary set of shutters using mechanical translation has been fabricated as a precursor to the VO_2 array. Fig. 5 shows the output spectral characteristics due to individual shutter elements at different positions along the array. The transmittance characteristics are those of a household plastic. The individual slits produce a similar spectrum that is linearly shifted along the output plane. In the actual coding, this spectral information is multiplexed together. An added benefit of the input multiplexing is that redundant data can be used to compensate for any dead pixels in the detector array. A second benefit is that the spectral range, for a given size of the detector array, can be expanded by about Ns/2 $\Delta\lambda_p$, where $\Delta\lambda_p$ is the spectral bandwidth corresponding to a single pixel. By tailoring the input shutter array spacing such that adjacent shutters shift the output spectrum by less than the width of the detector pixel, additional sampling points can be provided that can be used to improve the attainable spectral resolution for a given size of the detector array. This entails a trade-off between the gain in SNR and the improvement in spectral resolution due to the input optical coding.

Figures 5 and 6 show some preliminary results regarding the transmission accuracy as obtained using a single slit and that for multiplexing the data from 6 slits. The transmittance scale is expanded to show the signal ripple. Using data from a single slit, the ripple or noise on the transmittance data is about +/- 0.001 with 1.000 representing 100% transmittance. Using the data provided by 6 slits, the ripple could be reduced to below +/- 0.0002.

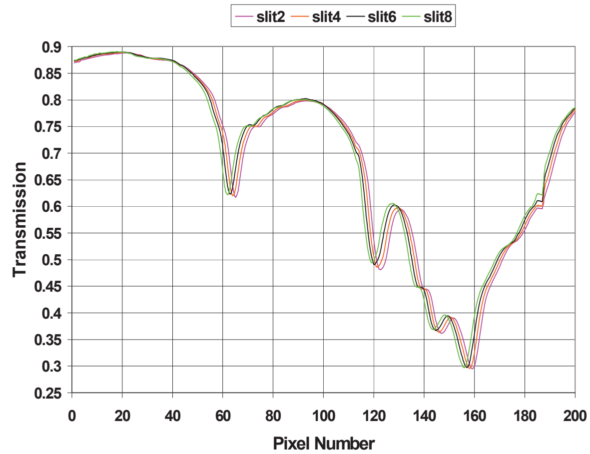

Fig. 5: Output transmission spectra of a plastic as measured with the IOSPEC spectrometer using different slit positions.

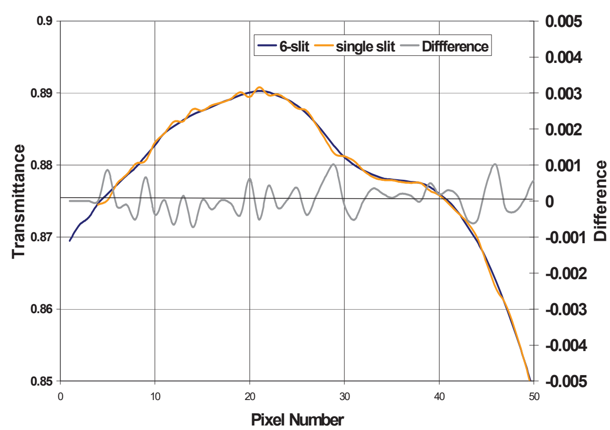

Fig. 6: Expanded view of a segment of the transmittance characteristic of the plastic shown in fig. 5 using data from a single slit and multiplexed using 6 slits.

The main benefits to the binary-coded IOSPEC spectrometer relative to the single slit spectrometer are:

1. Increase in input luminosity by a factor of $N_s/2$
2. Each detector pixel sees up to N_s wavelengths simultaneously.
3. $N_s^2/4$ sets of redundant data after each sequence of measurements to enable further signal averaging.
4. Linear spectral shift due to each slit facilitates improvement in spectral resolution.
5. Redundant data can be used to eliminate effects of dead pixels in linear array.
6. Binary coding enables a simple inverse transform.

Nonidealities in the coding mask, source intensity variations across the mask array, and nonidealities in the output imaging onto the detector array will reduce the attainable SNR relative to the ideal case. Nevertheless, a significant gain in SNR by a factor of 10 or more is possible. Examples of applications for the miniature optically-coded spectrometer include:

1- Gas monitoring (examples) - CO, CO_2, CH_4, NO, N_2O, SO_2, PH_3, AsH_3 - pollution monitoring - greenhouse gases
2- Atmospheric aerosols and dust that can affect weather patterns and precipitation
3- "Insitu" science experiments in space - evaluation of materials, monitoring of space experiments such as plant growth
4- Identification of minerals and planetary resources (I.e. rock type, ore content) geology
5- Detection of ice, water, bio-indicators and microbes (astrobiology)
6- Biohazard detection - manned missions
7- Monitoring of water or air quality - life-support systems for manned missions

4. COMPARISON WITH OTHER SPECTROMETERS

Table 4 compares the basic parameters of the IOSPEC miniature spectrometer, the improvements with the addition of the input coding array, and the basic characteristics of a typical FT-IR spectrometer. The size and mass quoted for IOSPEC is based on the current terrestrial model. It includes the input optics and the processing electronics. The spectrometer itself is only about 50 mm x 5 mm x 90 mm in size. Still further substantial reductions in size and weight of the module by at least 50% are possible.

As discussed in [6], many of the performance characteristics of the miniature IOSPEC integrated spectrometer; including the input NA (> 0.3), low detector NEP and high responsivity, low sensitivity to optical noise, and the maximum spectral scan rate (> 200 scans/s) can be superior to those of much larger and bulkier FT-IR instruments. Since the detector pixel size is miniaturized for coupling to the output of the IOSPEC spectrometer, the intrinsic NEP is smaller than that for the detector size typically employed by the much-larger bulk-optic FT-IR systems. IOSPEC also has the advantage that the entire spectrum is measured in parallel during each spectral scan to maximize the per pixel integration time. These factors help to compensate for the much smaller input aperture on the miniature spectrometer relative to the large bulk-optic systems.

Table 4: Spectrometer Performance Comparison

Parameter	IOSPEC	Coded IOSPEC	FT-IR
Input Aperture Size (A_i)	$w \bullet h_w$ = $0.006 \bullet h_w$ cm^2	$(N_t/2\text{-}1)w\bullet h_w$ cm^2, h_w unlimited	5.07 cm^2
Input Nume-rical Aperture	0.3 to 0.5	0.3 to 0.5	0.03
Input Lumino-sity (sr cm^2)	0.0018h	0.0018 h (N_H/2-1)	0.015
Net Internal Transmittance	0.2 to 0.4	0.2 to 0.4	about 0.34
Intrinsic Reso-lution ($\Delta\lambda/\lambda$)	> 1/5000	> 1/5000	1/15000
A_{det} (typical detector pixel size)	0.0375 mm^2	0.0375 mm^2	1.75 mm^2
Pixel Spectral Bandwidth	$\Delta\lambda_{CH}$ (~ 2 nm limit for m=1 60 µm slits)	$\Delta\lambda_{CH}$ (~2 nm limit for m=1, 60 µm slits)	~ 0.5 cm^{-1} in wavenumber
Equivalent Detector Responsivity (PbSe, 250 K)	$2\cdot 10^5$ V/W	$2\cdot 10^5$ V/W	$4.3\cdot10^3$ V/W
Detector per pixel integration time for f_s scan rate	$1/f_s$	$1/(N_H f_s)$	$1/(2Nf_s)$
NEP (Noise Equivalent Power)	$0.019f_s^{0.5}/D^*$	$0.019(N_H f_s^{0.5})/D^*$	$0.13(2Nf_s)^{0.5}/D^*$
Optical Noise	$(P_{is}+P_{iB})\Delta\lambda_{CH}$	$(P_{is}+P_{iB})\ \Delta\lambda_{CH}$	$(P_{is}+P_{iB})$ x $N\Delta\lambda_{CH}$
Full spectrum scan rates	Up to 1000 scans/sec	Up to 1000/N_H sans/sec.	Max. ~60 scans/sec
Weight	2 to 3 kg	2 to 3 kg	> 15 kg

Where, in table 4:

- D* is the detector specific detectivity,
- f_s is the scan rate,
- h_w is the height of the waveguide core,
- N(x2) is the number of sample points in Fourier space
- N_H is the number of Hadamard slits,
- P_{is} is the statistical or random variations in the source optical signal at a given λ,
- P_{iB} is the background optical signal within the spectrometer itself due to scattered light and thermal self-emission by the spectrometer optics.
- w is the width of the input slit,
- $\Delta\lambda_{CH}$ is the Pixel Spectral Bandwidth.

In terms of optical performance, the IOSPEC technology has no restrictions on the input slit height. However, the input slit width defines the resulting spectral resolution and limits the input luminosity. The addition of the binary input coding using a programmable area of thin-film smart-material shutters can provide the advantages of a FT-IR system without the disadvantages:

- mechanical simplicity with no moving parts,
- large input aperture and luminosity,
- binary-coded wavelength multiplexing for Felgett's SNR advantage and data redundancy,
- direct measurement of the spectral data
- exact, simple binary inverse transform,
- potential to increase the attainable spectral resolution relative to the number of pixels in the detector array.

Because only a fixed number of wavelengths are multiplexed onto a single pixel in the binary-coded IOSPEC system, comparable to the number of shutter elements in the shutter array, sensitivity to optical noise should be much lower for the coded IOSPEC system relative to FT-IR systems in which the detector sees the entire spectral background noise spectral bandwidth. The higher scan rate that is feasible for the IOSPEC system, exceeding 200 scans/sec, relative to a maximum of about 60 scans/sec for an FT-IR, helps to reduce noise due to signal and temperature fluctuations, and facilitates a larger number of scan averages in the same measurement time.

For the application of the monitoring of the air and water quality in recycled life-support systems in manned space systems, the IOSPEC system has a number of distinct advantages. Its minimal size and weight minimize penalties for incorporation into spacecraft. The direct measurement of the spectral information and exact binary inverse transform can facilitate higher accuracies in absolute transmittance measurement than is feasible using typical FT-IR systems. This also provides more CPU time for sample analysis and trace substance identification using stored spectral libraries. The lack of moving mechanical components provides high reliability and minimizes power requirements.

5. CONCLUSIONS

The IOSPEC technology using proprietary signal processing has extended the state-of-the-art for high accuracy infrared transmittance measurements by miniature spectrometers with a signal to noise exceeding 250,000 using cooled PbS detector pixels for the 1 to 3.5 μm range and a peak SNR exceeding about 25,000 using PbSe detector pixels. Total sample measurement times are typically under 60 sec. This has provided a measured resolution of the sample optical absorbance of better than +/- 0.00015 abs. units. These results were obtained using a 20 W lamp.

The integration of the IOSPEC IR spectrometer technology with advanced optical coding techniques and MEMS miniaturization technologies can provide a further order-of-magnitude improvement in the attainable performance for the next-generation IR spectrometers, while substantially minimizing the instrument mass, size and power requirements. This can enable a level of science on smaller space platforms such as microsat and planetary rover missions that approaches that of a terrestrial laboratory, enabling the accommodation of additional probes and specimen collection systems. Potential space applications of this technology include atmospheric studies of aerosols and dust, planetary hyperspectral geological surveys, integration with planetary landers and rovers, to provide "in situ" analysis of the planetary surface or subsurface core samples.

In summary, the proposed miniature "next-generation" spectrometer module features:

1- IOSPEC high-performance miniature integrated-waveguide spectrometer technology for broad-band (> 4000 nm) spectral measurements ($\Delta\lambda/\lambda$ < 1/5000).

2- Compact, monolithically integrated spectrometer module (< 4 kg, < 0.2 m x 0.2 m x 0.25 m including electronics).

3- Proprietary DCS dark current subtraction technology to extend IR detector dynamic range and thermal stability [6]

4- Proprietary Smart signal processing routine that provides greater than x10 improvement in attainable SNR with any detector array, reducing both random signal variations and systematic noise

5- Binary input coding using a thin-film programmable shutter array to provide additional:

x 10 or more increase in SNR
x 2 or more improvement in spectral resolution

With the addition of input optical signal coding using a programmable input shutter array fabricated using thin-film electrochromic materials, a further improvement in the SNR of a factor of 10 is feasible. Using simple sample concentration techniques, low ppb detectivities may be feasible, depending on the characteristics (i.e. optical absorption strength) of the trace substance.

ACKNOWLEDGMENTS

The authors would like to acknowledge the financial assistance of the Canadian Space Agency.

6. REFERENCES

1. M.J. Persky, A review of spaceborne infrared Fourier transform spectrometers for remote sensing," Rev. Sci. Instrum. **66**, pp. 4763-4797 (1995).
2. D. Helm, H. Labischinski, G. Schallehn and D. Naumann, J. Gen. Microbiol., **137**, pp. 69-79 (1991). T. Visser, "Infrared Spectroscopy in Environmental Analysis," in Encyclopedia of Analytical Chemistry, Ed. R.A. Meyers, J. Wiley & Sons, Chichester, 1999.
3. R. Beer and T.A. Glavich, "Remote Sensing of the Troposphere by Infrared Emission Spectroscopy; Advanced Optical Instrumentation for Remote sensing of the Earth's surface from Space," Proc. SPIE **1129**, pp. 42-51 (1989).
4. G.A. Vanasse and H. Sakai, 'Fourier Spectroscopy' in "Progress in Optics", ed. E.Wolf, vol. VI, North Holland Publishing, pp. 261-327 (1967).
5. T. Stuffler, M. Mosebach, D. Kampf, M. Glier, A. Honne and G. Tan, "Status Report on Anita, an FTIR Spectrometer Flight Experiment for Manned Space Cabin Air Analysis," SAE Proceedings of the 32nd International Conference on Environmental Systems, San Antonio, Texas, 2002, paper **01-2454**.
6. R.V. Kruzelecky, S. Paquet, A.K. Ghosh, C. Tremblay, J. Lauzon and N. Landry, in " Infrared Technology and Applications XXII", B.F. Andresen and M. S. Scholl, Eds., SPIE vol. **2744**, p. 684-695 (1996).
7. R.V. Kruzelecky and A.K. Ghosh, *Miniature Spectrometers*, in "Handbook of Vibrational Spectroscopy," vol. 1, eds. John Chalmers and Peter R. Griffiths, John Wiley & Sons, pp. 423-435 (2002).
8. N.J.A. Sloane, T. Fine and P.G. Philips, Optical Spectra, April, p. 50-53 (1970).
9. J.A. Decker, Appl. Opt., **10**, p 510 (1971).
10. R.M. Hammaker, R.A. DeVerse, D.N. Asunskis and W. G. Fateley, Hadamard Transform Near-Infrared Spectrometers, in "Handbook of Vibrational Spectroscopy," vol. 1, eds. John Chalmers and Peter R. Griffiths, John Wiley & Sons, 2002, p.p. 453-460.
11. C.H. Griffiths and H.K. Eastwood, J. Appl. Physics, **45**, p. 2201-2206 (1974).
12. G. Stefanovich, A Pergament and D. Stefanovich, J. Phys. Condens. Matter, **12**, p. 8837-8845 (2000).
13. R.V.Kruzelecky, E. Haddad, M. Soltani, M. Chaker and D. Nikanpour, Integrated Thin-Film Smart Coatings with Dynamically-Tunable Thermo-Optical Characteristics, SAE Proceedings of the 32nd International Conference on Environmental Systems, San Antonio, Texas, 2002, **02ICES-170**.

ACRYNOMS AND NOMENCLATURE

SYMBOL	DESCRIPTION
CSA	Canadian Space Agency
DCS	Dark Current Subtraction
DMA	Digital Micro-mirror Arrays
FT-IR	Fourier Transform Infrared
FWHM	Full Width Half Maximum
HT	Hadamard Transform I
IMS	Ion Mobility Spectroscopy
IOSPEC	MPB Integrated Optical SPECtrometer
IR	Infrared
MEMS	Micro Electro-mechanical Systems
MIS	Metal Insulator Semiconductor
NEP	Photodetector noise equivalent optical power for SNR=1.
N_s	Number of programmable shutters in input binary code array.
PbS	Lead Sulfide detector material (primarily for 1 to 5 μm spectral range).
PbSe	Lead Selenide detector material (primarily for 1 to 3.2 μm spectral range - dependent on detector operating temperature).
SNR	Signal to Noise Ratio
Vmeas	Measured voltage at output of detector preamplifier.
VIS	Visible
UV	Ultraviolet